

Contribution from the Departments of Chemistry, Louisiana State University, Baton Rouge, Louisiana 70803, and Tulane University, New Orleans, Louisiana 70118

Cyclometalated Complexes of Ruthenium. 2. Spectral and Electrochemical Properties and X-ray Structure of Bis(2,2'-bipyridyl)(4-nitro-2-(2-pyridyl)phenyl)ruthenium(II)

P. REVECO,[†] R. H. SCHMEHL,[‡] W. R. CHERRY,^{**} F. R. FRONCZEK,[†] and J. SELBIN^{**}

Received March 4, 1985

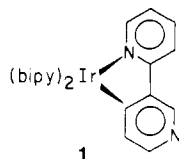
Several cyclometalated complexes of ruthenium(II), $[\text{Ru}(\text{bpy})_2\text{L}]^+$ (L = 2-(3-nitrophenyl)pyridine, phenylpyridine, benzo[*h*]quinoline, azobenzene, and *p*-(dimethylamino)azobenzene), have been prepared. The structural, electrochemical, and spectroscopic properties of one member of this series, L = 2-(3-nitrophenyl)pyridine, are reported. $[\text{RuC}_{31}\text{H}_{23}\text{N}_6\text{O}_2]\text{BF}_4 \cdot \frac{1}{2}\text{CH}_2\text{Cl}_2 \cdot \frac{1}{2}\text{H}_2\text{O}$ crystallizes in triclinic space group $P\bar{1}$ with $a = 9.004$ (2) Å, $b = 12.081$ (3) Å, $c = 14.970$ (4) Å, $\alpha = 86.62$ (2)°, $\beta = 78.15$ (2)°, $\gamma = 85.03$ (2)°, and $Z = 2$. The X-ray structure shows an unusually short Ru-C bond length, 1.997 (7) Å. The major perturbations resulting from cyclometalation are an increase in electron density around the metal atom and an increase in the crystal field strength. These changes are mirrored in the electrochemical and spectroscopic behavior of the cyclometalated complex, and this behavior is contrasted with that of the analogous $[\text{Ru}(\text{bpy})_3]^{2+}$ complex.

Introduction

Recent years have witnessed an explosive growth of interest in the photophysics and photochemistry of d^6 coordination complexes involving nitrogen heterocyclic ligands such as bipyridine (bpy) and its derivatives.¹ This intense interest results from the fact that this series of complexes constitutes one of the preeminent paradigms of inorganic photochemistry.² Indeed, many accepted and currently emerging theories in this area have been experimentally verified with the aid of d^6 polypyridine complexes.

In general, these investigations have centered around complexes of the type $[\text{M}(\text{bpy})_{3-x}\text{L}_x]^{n+}$, where $x = 1-3$ and L is typically some type of bidentate, nitrogen donor ligand. Recently, however, some cyclometalated counterparts of these complexes have been prepared and their physical properties reported.^{3,4} Such complexes display promise in expanding our understanding of inorganic excited-state processes for several reasons. First, replacement of a nitrogen donor by an effectively carbanion donor will drastically alter the electron density around the metal atom. This translates into substantial variations in both ground- and excited-state redox properties. Second, the carbanion donor is much higher in the spectrochemical series than the corresponding nitrogen donor. Consequently, any ligand field (LF) excited states will occur at higher energies for the cyclometalated complex; this may result in substantial perturbations of photophysical and photochemical properties.

Many cyclometalated complexes involving ligands that contain a phenyl group adjacent to a good ligating functionality are known.⁴ Furthermore, Watts and co-workers have observed cyclometalation even in the case of bpy.³ When Ir(III) reacts with bpy, a product is isolated in which one bpy is coordinated to the metal atom through a N atom of one ring and the C3 atom of the other ring (1).



In order to evaluate the effect of cyclometalation upon both the ground- and excited-state physical and chemical properties, we have prepared and spectroscopically investigated the first examples of related cyclometalated complexes of Ru(II), $[\text{Ru}(\text{bpy})_2\text{L}]^+$, where L is an aromatic ortho-metaling species such as 2-phenylpyridine (PP), 2-(3-nitrophenyl)pyridine (NPP), azobenzene (AB), *p*-(dimethylamino)azobenzene (DAB), and benzo[*h*]quinoline (BQ). Previously, the preparation and 400-MHz two-dimensional proton NMR study of $[\text{Ru}(\text{bpy})_2(\text{NPP})]^+$ have been detailed.⁵ In the present work, the X-ray crystal structure, electrochemical and spectral (absorption, emission)

properties, and the photochemistry of $[\text{Ru}(\text{bpy})_2(\text{NPP})]^+$ are reported.⁶

Experimental Section

The preparation of the cation $[\text{Ru}(\text{bpy})_2(\text{NPP})]^+$ as either the BF_4^- or PF_6^- salt has been described.⁵ All solvents were purified by standard methods.⁷

X-ray Structure. Intensity data were collected on a very dark red needle of dimensions $0.10 \times 0.20 \times 0.64$ mm by using an Enraf-Nonius CAD4 diffractometer equipped with Mo $K\alpha$ radiation ($\lambda = 0.71073$ Å) and a graphite monochromator. The ω - 2θ scans were made at rates varying from 0.74 to $5.0^\circ \text{ min}^{-1}$ in order to measure all significant data with $I \approx 25\sigma(I)$. Crystal data: $[\text{RuC}_{31}\text{H}_{23}\text{N}_6\text{O}_2]\text{BF}_4 \cdot \frac{1}{2}\text{CH}_2\text{Cl}_2 \cdot \frac{1}{2}\text{H}_2\text{O}$, fw = 750.9, triclinic space group $P\bar{1}$, $a = 9.004$ (2) Å, $b = 12.081$ (3) Å, $c = 14.970$ (4) Å, $\alpha = 86.62$ (2)°, $\beta = 78.15$ (2)°, $\gamma = 85.03$ (2)°, $V = 1586$ (1) Å³, $Z = 2$, $d_{\text{calcd}} = 1.572$ g cm^{-3} , $\mu(\text{Mo } K\alpha) = 6.31$ cm^{-1} , $T = 26^\circ \text{C}$. One hemisphere of data was collected within $2^\circ < 2\theta < 43^\circ$. Data reduction included corrections for Lorentz, polarization, background, and absorption effects. The latter were based upon ψ scans of reflections near $\chi = 90^\circ$, and the minimum relative transmission coefficient was 97.17%. Of the 3641 unique data, 2549 had $I > 3\sigma(I)$ and were used in the refinement.

The structure was solved by heavy-atom methods and refined by full-matrix least squares based on F with weights $w = \sigma^{-2}(F_o)$, treating non-hydrogen atoms anisotropically. Hydrogen atoms were included as fixed contributions in calculated positions with isotropic $B = 5.0$ Å² (10.0 Å² for CH_2Cl_2). Solvent molecules CH_2Cl_2 and H_2O were located across a center of symmetry at 0, $1/2$, $1/2$. Populations of $1/2$ were assigned to all atoms in these molecules, and this model caused no problems in least squares, as the disorder was well resolved.

All computations were carried out by using the Enraf-Nonius SDP.⁸ Scattering factors were those of Cromer and Waber,⁹ anomalous coef-

- (1) The literature in this field is too voluminous to enumerate here, but the reader is referred to the following reviews for pertinent references: Watts, R. J. *J. Chem. Educ.* **1983**, *60*, 834. Seddon, K. R. *Coord. Chem. Rev.* **1982**, *41*, 79. Kalyanasundaram, K. *Ibid.* **1982**, *41*, 159. See also: Steel, P. J.; Lahousse, F.; Lerner, D.; Marzin, C. *Inorg. Chem.* **1983**, *22*, 1488. Rillema, D. P.; Allen, G.; Meyer, T. J.; Conrad, D. *Ibid.* **1983**, *22*, 1617. Cherry, W. R.; Henderson, L. J., Jr. *Ibid.* **1984**, *23*, 983 and references therein.
- (2) Geoffroy, G. L.; Wrighton, M. S. "Organometallic Photochemistry"; Academic Press: New York, 1979. Adamson, A. W.; Fleischauer, P. D. "Concepts of Inorganic Photochemistry"; Wiley-Interscience: New York, 1983, 1975; *J. Chem. Educ.* **1983**, *60*, 784-887.
- (3) Watts, R. J.; Harrington, J. S.; Van Houten, J. *J. Am. Chem. Soc.* **1977**, *99*, 2179. Wickramasinghe, W. A.; Bird, P. H.; Serpone, N. *J. Chem. Soc., Chem. Commun.* **1981**, 1284. Nord, G.; Hazell, A. C.; Hazell, R. G.; Farver, O. *Inorg. Chem.* **1983**, *22*, 3429. Spellane, P. J.; Watts, R. J.; Curtis, C. J. *Ibid.* **1983**, *22*, 4060.
- (4) Nanoyama, M. *Bull. Chem. Soc. Jpn.* **1974**, *47*, 767. Nanoyama, M.; Yamasaki, K. *Inorg. Nucl. Chem. Lett.* **1971**, *7*, 943. Yin, C. C.; Deeming, A. J. *J. Chem. Soc., Dalton Trans.* **1975**, 2091. Hiraki, K.; Obayashi, Y.; Oki, Y. *Bull. Chem. Soc. Jpn.* **1979**, *52*, 1372. Bruce, M. I.; Goodall, B. L.; Stone, G. A. *J. Organomet. Chem.* **1973**, *60*, 343.
- (5) Reveco, P.; Medley, J. H.; Garber, A. R.; Bhacca, N. S.; Selbin, J. *Inorg. Chem.* **1985**, *24*, 1096.
- (6) Results for the remaining complexes will be reported in a forthcoming paper: Reveco, P.; Cherry, W. R.; Selbin, J., submitted for publication in *Inorg. Chem.*
- (7) Gordon, S. A. J.; Ford, R. A. "The Chemist's Companion"; Wiley: New York, 1972.
- (8) Frenz, B. A.; Okaya, Y. "Enraf-Nonius Structure Determination Package"; Enraf-Nonius: Delft, Holland, 1980.

[†]Louisiana State University.

[‡]Tulane University.

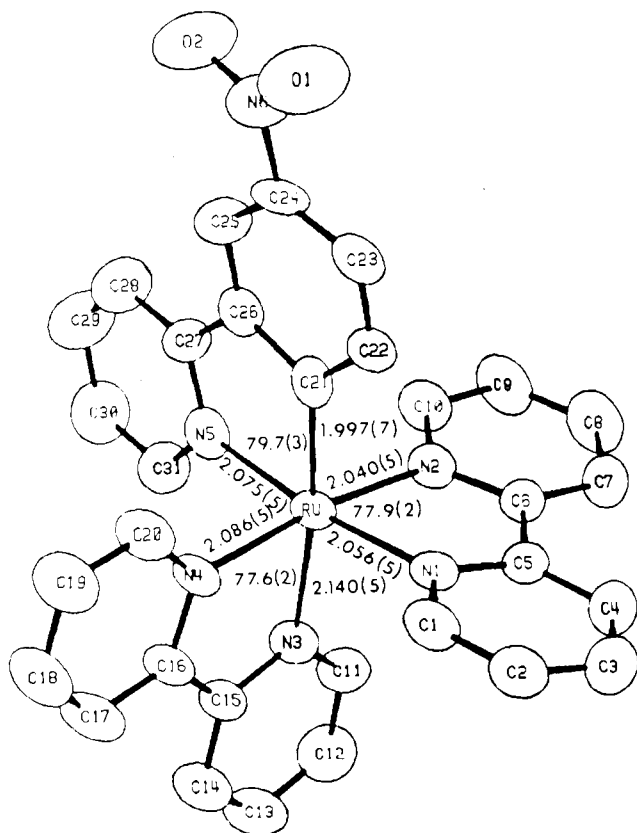


Figure 1. Crystal structure of $[\text{Ru}(\text{bpy})_2(\text{NPP})]^+\text{BF}_4^-$.

ficients were those of Cromer.¹⁰ Final $R = 0.046$ and $R_w = 0.052$.

Electrochemistry. Electrochemical measurements were made on dilute (5×10^{-4} M) dichloromethane solutions (0.1 M in tetrabutylammonium perchlorate (TBAP) supporting electrolyte) by using a three-electrode system. A platinum-wire working electrode and counter electrode were used, along with a pseudo reference electrode of silver wire-dichloromethane solution that is 0.1 M in TBAP. The potentials of the pseudo reference electrode vs. the saturated sodium chloride calomel electrode (SCE) were measured at the end of each run. The wave form generators and potentiostats for the cyclic voltammetry experiments were a Pine Instrument Co. Model RDE for lower scan rates and a Princeton Applied Research Model 174A polarographic analyzer for fast scans. Cyclic voltammograms were recorded on a Hewlett-Packard Model 7044A X-Y recorder.

Absorption and Emission Spectra. Absorption spectra were recorded on a Cary 14 spectrometer. The emission spectra were recorded on an SLM-4800S spectrofluorometer and corrected for photomultiplier response. The relative emission intensities were determined for each sample in a 6-mm-i.d. Pyrex tube after several freeze/pump/thaw degassing cycles. The temperature was maintained by adjusting the flow of pre-cooled nitrogen gas. The sample temperature was monitored with a copper/constantan thermocouple.

The relative quantum yields were converted into absolute quantum yields by using $[\text{Ru}(\text{bpy})_3]^{2+}$ as the standard. The lifetime of $[\text{Ru}(\text{bpy})_3]^{2+}$ over the temperature range of 77–250 K has been evaluated.¹¹ The emission quantum yield for this complex was then determined at 120 K by using the lifetime and radiative rate constant. This procedure may introduce some systematic error so that quantitative arguments are best based upon the temperature dependence of the emission lifetime.

Lifetimes. Luminescence lifetime measurements were obtained by using pulsed nitrogen laser excitation with pulses at 337 nm and a 350-ps width. Emission was observed at right angles by a Hamamatsu R777 photomultiplier through a monochromator system. Time-resolved detection was accomplished by computerized scanning of a gated integrator.

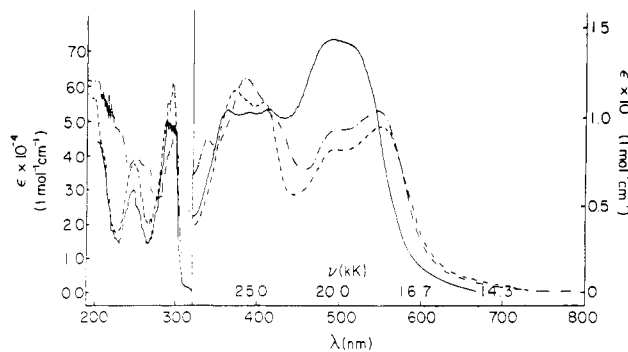


Figure 2. Absorption spectra for $[\text{Ru}(\text{bpy})_2\text{L}]^+$ in methanol. L = NPP (—), L = PP (---), and L = BQ (···).

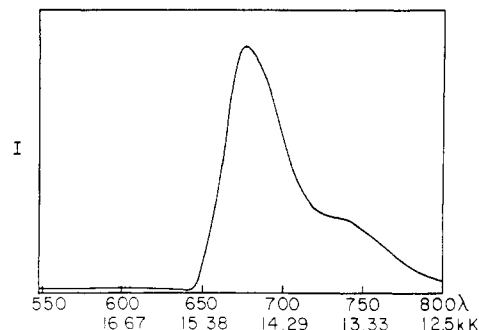


Figure 3. Emission spectrum of $[\text{Ru}(\text{bpy})_2(\text{NPP})]^+$ in EtOH/MeOH (4:1) at 77 K.

A more complete description of the lifetime apparatus is presented elsewhere.¹²

Photochemistry. The photoanation progress was monitored by absorption spectroscopy using a Cary 14 spectrometer. A locally constructed cell holder allowed for sample stirring, temperature control, and right-angle irradiation. The sample temperature was maintained at $23 \pm 1^\circ\text{C}$ as measured by a copper/constantan thermocouple.

Results

The crystal structure for $[\text{Ru}(\text{bpy})_2(\text{NPP})]\text{BF}_4$ is shown in Figure 1. The atomic coordinates are displayed in Table I.

The absorption spectra for $[\text{Ru}(\text{bpy})_2\text{L}]^+$ (L = NPP, PP, and BQ) are shown in Figure 2. The latter two spectra are presented for comparison. The emission spectrum of $[\text{Ru}(\text{bpy})_2(\text{NPP})]^+$ is shown in Figure 3. This spectrum was obtained at 77 K in an EtOH/MeOH (4:1) glass. This spectrum resembles that of $[\text{Ru}(\text{bpy})_3]^{2+}$ in that vibrational fine structure is apparent. However, the emission maximum is substantially bathochromically shifted in the case of $[\text{Ru}(\text{bpy})_2(\text{NPP})]^+$ (Table II).

The quantum yield and emission lifetime for $[\text{Ru}(\text{bpy})_2(\text{NPP})]^+$ were evaluated as 0.038 and 898 ns, respectively, at 77 K. Both of these properties were very dependent upon the temperature. Figure 4 shows the temperature dependence for the emission intensity. As reported in previous cases,^{11,13} this temperature dependence could be described by eq 1, where the rate constants are as defined in Figure 5. The best fits to eq 1 are shown in Table II.

$$k_{\text{exptl}} = 1/\tau = k_r + k_{\text{nr}} + k_0 e^{-\Delta E/RT} = k + k_0 e^{-\Delta E/RT} \quad (1)$$

$$\phi^{-1} = k_{\text{exptl}}/k_r = k/k_r + (k_0/k_r) e^{-\Delta E/RT}$$

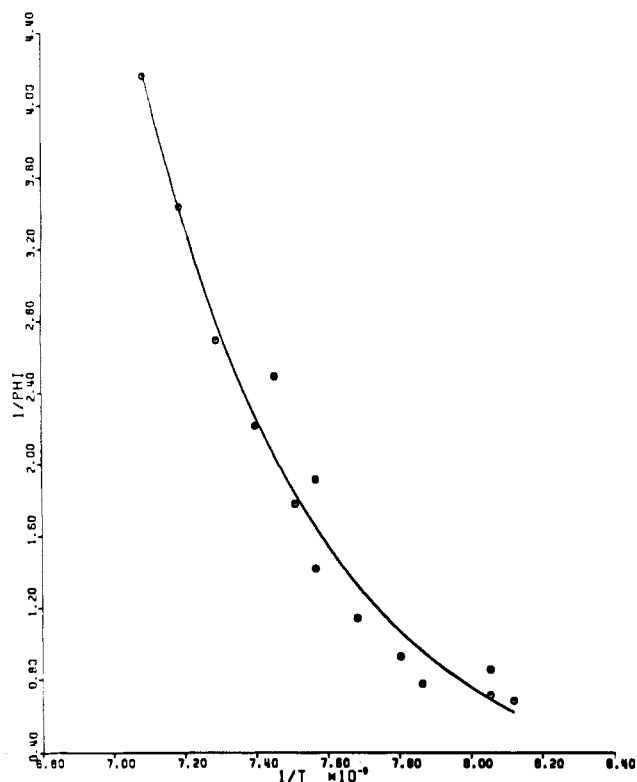
The oxidation potential of $[\text{Ru}(\text{bpy})_2(\text{NPP})]^+$ was evaluated as 0.776 V relative to SCE in CH_2Cl_2 for this completely reversible process. (This is well below the 1.29 V found for $[\text{Ru}(\text{bpy})_3]^{2+}$.)

- (9) Cromer, D. T.; Waber, J. T. "International Tables for X-ray Crystallography"; Kynoch Press: Birmingham, England, 1974; Vol. IV, Table 2.2B.
- (10) Cromer, D. T. "International Tables for X-ray Crystallography"; Kynoch Press: Birmingham, England, 1974; Vol. IV, Table 2.3.1.
- (11) Borjellei, F.; Juris, A.; Balzani, V.; Belzer, P.; von Zelewsky, A. *Inorg. Chem.* **1983**, *22*, 3335.

- (12) Wacholtz, W.; Auerbach, R. A.; Schmehl, R., manuscript in preparation.
- (13) Kemp, T. J. *Prog. React. Kinet.* **1980**, *10*, 301. Van Houten, J.; Watts, R. J. *J. Am. Chem. Soc.* **1976**, *98*, 4853. Durham, B.; Caspar, J. V.; Nagle, J. K.; Meyer, T. J. *Ibid.* **1982**, *104*, 4803. Allsopp, S. R.; Cox, A.; Kemp, T. J.; Reed, W. J. *J. Chem. Soc., Faraday Trans. 1* **1978**, *74*, 1275.

Table I. Coordinates for $[(\text{bpy})_2\text{Ru}(\text{C}_{11}\text{H}_7\text{N}_2\text{O}_2)]\text{BF}_4 \cdot 1/2\text{CH}_2\text{Cl}_2 \cdot 1/2\text{H}_2\text{O}$

atom	x	y	z	atom	x	y	z
Ru	0.05467 (8)	0.21539 (6)	0.22139 (5)	C17	0.2686 (11)	0.2299 (9)	0.4526 (6)
O1	0.5580 (9)	0.3947 (7)	-0.1659 (6)	C18	0.3971 (11)	0.2724 (10)	0.4203 (6)
O2	0.4292 (9)	0.5473 (6)	-0.1284 (5)	C19	0.4392 (11)	0.3036 (10)	0.3296 (7)
N1	0.1264 (7)	0.0515 (5)	0.1979 (4)	C20	0.3392 (10)	0.2887 (8)	0.2742 (6)
N2	-0.1030 (7)	0.1680 (5)	0.1539 (4)	C21	0.1786 (9)	0.2766 (7)	0.1058 (5)
N3	-0.0628 (7)	0.1648 (6)	0.3547 (4)	C22	0.2842 (9)	0.2216 (7)	0.0386 (5)
N4	0.2078 (7)	0.2445 (6)	0.3032 (4)	C23	0.3716 (9)	0.2744 (8)	-0.0352 (5)
N5	-0.0236 (7)	0.3820 (6)	0.2284 (4)	C24	0.3527 (10)	0.3888 (7)	-0.0428 (5)
N6	0.4530 (9)	0.4454 (6)	-0.1173 (5)	C25	0.2464 (10)	0.4491 (7)	0.0171 (6)
C1	0.2520 (9)	-0.0049 (8)	0.2196 (6)	C26	0.1566 (9)	0.3933 (7)	0.0905 (5)
C2	0.2858 (11)	-0.1160 (8)	0.2074 (6)	C27	0.0403 (9)	0.4497 (7)	0.1570 (6)
C3	0.1890 (12)	-0.1748 (8)	0.1735 (7)	C28	-0.0110 (12)	0.5604 (8)	0.1544 (7)
C4	0.0622 (11)	-0.1182 (7)	0.1490 (6)	C29	-0.1234 (12)	0.6012 (9)	0.2197 (8)
C5	0.0341 (9)	-0.0073 (7)	0.1616 (5)	C30	-0.1866 (12)	0.5341 (9)	0.2939 (7)
C6	-0.0945 (9)	0.0603 (7)	0.1344 (5)	C31	-0.1331 (10)	0.4229 (8)	0.2954 (6)
C7	-0.2008 (10)	0.0183 (7)	0.0931 (6)	B	0.3670 (12)	0.1356 (10)	0.6863 (7)
C8	-0.3144 (10)	0.0884 (9)	0.0677 (7)	F1	0.3522 (8)	0.1663 (6)	0.7757 (4)
C9	-0.3214 (10)	0.1991 (9)	0.0856 (6)	F2	0.2222 (7)	0.1279 (6)	0.6721 (4)
C10	-0.2143 (9)	0.2374 (8)	0.1273 (6)	F3	0.4366 (9)	0.2157 (7)	0.6316 (5)
C11	-0.1965 (10)	0.1244 (7)	0.3764 (6)	F4	0.4483 (8)	0.0362 (6)	0.6741 (6)
C12	-0.2652 (11)	0.0941 (9)	0.4639 (7)	C11S ^a	0.3715 (14)	0.5581 (8)	0.4725 (6)
C13	-0.1910 (13)	0.1065 (9)	0.5328 (6)	C12S ^a	0.1500 (16)	0.5794 (12)	0.3749 (10)
C14	-0.0499 (11)	0.1460 (9)	0.5127 (6)	C1S ^a	0.3234 (28)	0.6097 (20)	0.3848 (15)
C15	0.0150 (10)	0.1741 (7)	0.4227 (5)	O1S ^a	-0.0777 (38)	0.4624 (28)	0.5400 (23)
C16	0.1648 (9)	0.2168 (7)	0.3937 (5)				

^a Population = 1/2.**Figure 4.** Temperature dependence of the emission intensity of $[\text{Ru}(\text{bpy})_2(\text{NPP})]^+$ in EtOH/MeOH (4:1). The solid curve is the computer-generated fit using the parameters in Table II.

The photochemical behavior of $[\text{Ru}(\text{bpy})_2(\text{NPP})]^+$ was evaluated in several different solvents. In CH_2Cl_2 containing 0.01 M tetrabutylammonium chloride $[(\text{TBA})\text{Cl}]$, in H_2O , and in aqueous 0.1 M NaCl, no change could be detected even after prolonged irradiation. In aqueous 0.1 M HCl, the complex was thermally unstable, decomposing to $[\text{Ru}(\text{bpy})_2(\text{H}_2\text{O})_2]^{2+}$ over the time span of several minutes. No increased rate was noted upon photolysis.

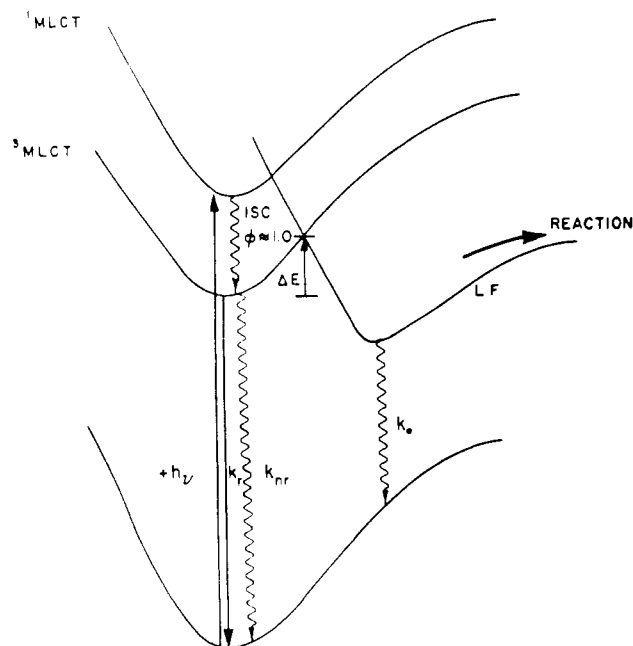
Discussion

X-ray Crystal Structure. The structure of the cation, illustrated in Figure 1, is one in which the Ru atom is coordinated in a

Table II. Comparison of Photophysical Properties of $[\text{Ru}(\text{bpy})_2\text{NPP}]^+$ and $[\text{Ru}(\text{bpy})_3]^{2+}$

	$[\text{Ru}(\text{bpy})_2\text{NPP}]^+$		$[\text{Ru}(\text{bpy})_3]^{2+}$ ^a	
abs max, nm	495 ^b		452	
emission				
λ_{max} , nm	682 ^c		583	
τ , ns	878		5200	
temp dependence				
	L ^d	Q ^d	L ^d	Q ^d
k^e	1.2×10^6	1.2×10^{-1}	3.9×10^5	7.9
k_0^e	2.6×10^{11}	6.7×10^6	1.9×10^{14}	1.6×10^9
ΔE , cm ⁻¹	956	1404	3859	3951

^a Much of these data has been reported previously,¹ but the reported values were evaluated as a check on procedures. These values agree with the literature. ^b In methanol at room temperature. ^c In 4:1 ethanol/methanol at 77 K. ^d L = based upon lifetime measurements; Q = based upon intensity measurements. ^e Units: L, s⁻¹; Q, unitless.

**Figure 5.** Photophysics of $[\text{Ru}(\text{bpy})_3]^{2+}$.

distorted octahedron with twist angle 51.1° . The five pyridine rings are individually planar to 0.018 (7) Å or better, and the two bipyridyls exhibit dihedral angles of 4.6° (N1, N2) and 3.1° (N3, N4) between their component rings. The metalated phenyl ring is less planar, having maximum deviation 0.033 (8) Å for the coordinated atom C21. The phenyl ring forms dihedral angles of 7.4° with the pyridine plane and 7.0° with the plane of the nitro group to which it is bonded.

The Ru–C bond length, 1.997 (7) Å, appears to be quite short when compared to a calculated single-bond distance. The magnitude of this shortening can be estimated by comparing the Ru–N and Ru–C bond lengths with the corresponding atomic radii. The N(sp²) radius is (from N(sp²)–C(sp³) = 1.475 Å and C(sp³)–C(sp³) = 1.537 Å) 0.707 Å.¹⁴ Likewise (since C(sp²)–C(sp³) = 1.510 Å), the C(sp²) radius is 0.742 Å. The Ru–C bond length is then expected to be (2.079 Å (average Ru–N distance) + 0.035 Å (larger C(sp²) radius)) 2.114 Å.¹⁵ Thus, the bond shortening is evaluated as 0.117 Å. This value is quite substantial compared to calculated metal–C(sp²) shortenings of 0.10 Å in the palladium(II) compound of the same cyclometalating ligand, [Pd(N-PP)(C₂H₃O₂)₂],¹⁶ and of 0.05 Å in the rhodium(III) compound [Rh(NPP)₂Cl]₂.¹⁷

The BF₄⁻ anion is tetrahedral with an average B–F distance of 1.364 (17) Å and an average F–B–F angle of 109.5 (17)°.

Excited-State Properties. The absorption spectrum of [Ru-(bpy)₂(NPP)]⁺ in methanol is shown in Figure 2. Four major bands can be observed; these are centered at 495 , 385 , 290 , and 245 nm. The latter two are similar to absorption bands of the free ligands and consequently may be assigned as intraligand (π – π^*) transitions, in the same way they have been assigned in the case of the bipyridine complexes.¹⁸

The absorption band centered at 495 nm is very intense ($\epsilon \sim 15000$ M⁻¹ cm⁻¹) and is in a region characteristic of metal-to-ligand charge-transfer (MLCT) (d – π^*) transitions for related complexes. Furthermore, the asymmetric nature of the band suggests that more than just one electronic transition may be involved. In fact, the electrochemical data as well as the results from related complexes shown in Figure 2 indicate that this band is actually due to at least two MLCT transitions, one localized on the bpy ligand and the other on the NPP ligand. The bathochromic shift in the Ru → bpy MLCT band relative to the equivalent band in [Ru(bpy)₃]²⁺ ($\lambda_{\max} = 450$ nm) is due to changes in the metal-centered t_{2g} orbital. The replacement of a nitrogen donor ligand by a carbon donor ligand (carbanion) greatly increases the electron density around the metal atom. This raises the energies of the d orbitals as is witnessed by the dramatic decrease in the oxidation potential of [Ru(bpy)₂(NPP)]⁺ relative to [Ru(bpy)₃]²⁺ (see Table II). From the proximity of the two MLCT transitions, the π^* orbitals of bpy and NPP apparently lie at nearly identical energies.

Finally, the absorption band(s) centered near 385 nm are quite intense and also are apparently due to MLCT transitions. Previously, this transition in [Ru(bpy)₃]²⁺ has been assigned as t_{2g} → $\pi^*(2)$ MLCT.¹⁹ This seems a reasonable assignment for the case at hand.

The emission spectrum for [Ru(bpy)₂(NPP)]⁺ in an EtOH/MeOH (4:1) glass at 77 K is displayed in Figure 3. The fact that the emission maximum occurs at 682 nm (compare [Ru(bpy)₃]²⁺ with $\lambda_{\max} = 583$ nm) is consistent with the bathochromic shift noted in the absorption spectrum. Indeed, the magnitudes of the

observed bathochromic shifts are similar for the absorption and emission spectra (1921 and 2520 cm⁻¹, respectively). The emission spectrum also displays the vibrational fine structure characteristic of Ru → bpy MLCT emission bands. In light of these facts, the emission may reasonably be assigned as an MLCT transition localized primarily on the bpy ligand. Similarly localized emissions have been reported previously.^{11,20}

Both the emission intensity and lifetime are extremely sensitive to temperature, as is shown in Figure 4. Similar behavior has been previously noted and has been quantitatively described by eq 1.^{11,13} The same approach has been utilized in the present case, and the computer-generated function of the emission intensity is shown in Figure 4. Clearly, these equations adequately describe the experimental data.

For previous polypyridine Ru(II) complexes, the above behavior has been attributed to population of a higher lying ligand field state (see Figure 5).^{13,21} This assignment is based primarily on the occurrence of photoanation as the high-lying state is populated. In the present case, this state is populated with unit efficiency at 298 K, yet no photoanation could be observed even in 0.01 M Cl⁻ (CH₂Cl₂), a medium where [Ru(bpy)₃]²⁺ undergoes photoanation very efficiently.²² Consequently, the observed temperature dependence must be related to an alternative process. One possibility is population of a higher lying triplet MLCT state that contains a significant amount of singlet character due to spin-orbit coupling. This state has been recently discussed by Meyer and Kober.²³

In the case of Ru(II), mixed complexes of bpy and either bipyrazine (bpyz) or bipyrimidine (bpyim) display temperature-dependent emission quantum yields and lifetimes but do not undergo photoanation when the higher state is populated.²³ Furthermore, the kinetic parameters for population of this state ($k_0 \sim 10^9$, $\Delta E \sim 400$ – 800 cm⁻¹) are considerably different from those obtained for population of the photoactive (LF) state ($k_0 \sim 10^{13}$, $\Delta E \sim 3000$ cm⁻¹). This discrepancy leads to the postulation of the higher lying ³MLCT with significant singlet character.

For the case at hand, the expected variations of the MLCT and LF energies support the assignment of the higher lying state as an ³MLCT state with significant singlet character. The energy separation between the ³MLCT and LF states in [Ru(bpy)₃]²⁺ has been experimentally evaluated as 3600 cm⁻¹.¹³ For [Ru-(bpy)₂(NPP)]⁺, MLCT states occur at lower energies relative to [Ru(bpy)₃]²⁺; witness the bathochromic shift in the absorption and emission maxima. On the other hand, LF states are expected to undergo hypsochromic shifts since a carbanion donor ligand is substantially higher than a nitrogen donor ligand in the spectrochemical series.² Consequently, the energy difference between the ³MLCT and LF states is expected to increase in [Ru-(bpy)₂(NPP)]⁺ relative to [Ru(bpy)₃]²⁺. Indeed, this larger ³MLCT/LF energy gap decreases the probability of LF population, which is most likely why population of the higher lying ³MLCT state can be observed.

Acknowledgment. P.R. wishes to thank Universidad Tecnica Federico Santa Maria, Valparaiso, Chile, for study leave. R.H.S. wishes to thank the donors of the Petroleum Research Fund, administered by the American Chemical Society, for partial support of this work. W.R.C. acknowledges support of the NSF (Grant CHE-8205698) and the LSU Center for Energy Studies, under U.S. Department of Energy Grant No. DE-FG-0580ER1019F. The authors wish to thank Professor R. J. Watts for helpful discussions and Professor T. J. Meyer for a preprint of ref 23.

(14) "International Tables for X-ray Crystallography"; Kynoch Press: Birmingham, England, 1968; Vol. 3, pp 270–276.

(15) Stynes, H. C.; Ibers, J. A. *Inorg. Chem.* **1971**, *10*, 2304.

(16) Selbin, J.; Abboud, K.; Watkins, S. F.; Gutierrez, M. A.; Fronczek, F. R. *J. Organomet. Chem.* **1983**, *241*, 259.

(17) Fronczek, F. R.; Gutierrez, M. A.; Selbin, J. *Cryst. Struct. Commun.* **1982**, *11*, 1119.

(18) Lytle, F. E.; Hercules, D. M. *J. Am. Chem. Soc.* **1969**, *91*, 253. Crosby, G. A. *Acc. Chem. Res.* **1975**, *8*, 231. Balzani, V.; Boletta, F.; Gandolfi, M. T.; Maestri, M. *Top. Curr. Chem.* **1978**, *75*, 1.

(19) Bryant, G. M.; Fergusson, J. E.; Powell, H. K. *J. Aust. J. Chem.* **1971**, *24*, 257.

(20) Anderson, S.; Seddon, K. R.; Wright, R. D.; Cocks, A. T. *Chem. Phys. Lett.* **1980**, *71*, 220. Klassen, D. M. *Ibid.* **1982**, *93*, 383.

(21) Van Houten, J.; Watts, R. J. *Inorg. Chem.* **1978**, *17*, 3381. Caspar, J. V.; Meyer, T. J. *J. Am. Chem. Soc.* **1983**, *105*, 5583. Demas, J. N.; Taylor, D. G. *Inorg. Chem.* **1979**, *18*, 3177.

(22) Gleria, M.; Minto, F.; Baggiato, G.; Bortolus, P. *J. Chem. Soc., Chem. Commun.* **1978**, 285.

(23) Meyer, T. J.; Kober, E. M. *Inorg. Chem.*, submitted for publication. This concept has been discussed in: Allen, G. H.; White, R. P.; Rillema, D. P.; Meyer, T. J. *J. Am. Chem. Soc.* **1984**, *106*, 2613.

Registry No. [Ru(bpy)₂(NPP)]BF₄, 98690-23-4; [Ru(bpy)₂(NPP)]-BF₄·1/2CH₂Cl₂·1/2H₂O, 98690-24-5; [Ru(bpy)₂(NPP)]⁺, 98690-22-3; [Ru(bpy)₂(PP)]⁺, 98690-25-6; [Ru(bpy)₂(BQ)]⁺, 98690-26-7; [Ru(bpy)₂(H₂O)₂]²⁺, 20154-62-5; [Ru(bpy)₃]²⁺, 15158-62-0.

Supplementary Material Available: Tables of bond distances, bond angles, coordinates for H atoms, anisotropic thermal parameters, and structure factor amplitudes (16 pages). Ordering information is given on any current masthead page.

Contribution from the Departments of Chemistry, Colorado State University, Fort Collins, Colorado 80523, University of Colorado at Denver, Denver, Colorado 80202, and University of Denver, Denver, Colorado 80208

Crystal and Molecular Structure of a Six-Coordinate Zinc Porphyrin: Bis(tetrahydrofuran)(5,10,15,20-tetraphenylporphinato)zinc(II)

CYNTHIA K. SCHAUER,^{1a} OREN P. ANDERSON,^{*1a} SANDRA S. EATON,^{*1b} and GARETH R. EATON^{*1c}

Received March 11, 1985

The crystal and molecular structure of a six-coordinate zinc porphyrin, bis(tetrahydrofuran)(5,10,15,20-tetraphenylporphinato)zinc(II) (**1**), was determined. The compound crystallized in *P* $\bar{1}$ (*Z* = 1), with *a* = 9.572 (1) Å, *b* = 11.115 (2) Å, *c* = 11.720 (3) Å, α = 102.71 (2)°, β = 103.78 (2)°, and γ = 115.01 (1)°. The structural model was refined to *R* = 0.040 (*R*_w = 0.043) for 3178 reflections with *I* > 2σ(*I*). The zinc atom was found precisely in the mean porphyrin plane of the centrosymmetric molecule (Zn–N = 2.056 (2), 2.058 (2) Å) and was only weakly bound to the THF molecules (Zn–O = 2.380 (2) Å). Crystals of **1** have been used as hosts for single-crystal EPR studies of metalloporphyrins bearing nitroxyl radical substituents. An analysis of the "free space" in the lattice of **1** shows that to accommodate a nitroxyl-substituted metalloporphyrin, THF must be lost from a neighboring unsubstituted Zn(TPP)(THF)₂ moiety.

Introduction

The relatively large size of the zinc(II) ion has been thought to preclude a zinc atom position in the mean porphyrin plane for zinc porphyrin complexes.²⁻⁵ Spectroscopic^{3,5} and binding constant⁴ studies have supported this view and have not yielded any evidence for the existence of six-coordinate zinc porphyrins in solution. No six-coordinate zinc porphyrin has been structurally characterized, and the only zinc porphyrin in which the metal atom occupies a position in the porphyrin plane (as it would in a symmetric six-coordinate species) is the four-coordinate Zn(TPP) complex (TPP = 5,10,15,20-tetraphenylporphyrin) in [Zn(TPP)]·2C₆H₅CH₃.⁶

In a donor solvent such as THF, or in the presence of added ligands, zinc(II) porphyrins apparently exhibit a preference for a five-coordinate structure which is similar to that of high-spin iron(II) porphyrins.⁷ High-spin iron(II) atoms were once thought to be too large to reside in the porphyrin plane, but the structural characterization of bis(tetrahydrofuran)(5,10,15,20-tetraphenylporphinato)iron(II) altered that belief.⁸ The crystal and molecular structure of the analogous six-coordinate zinc compound bis(tetrahydrofuran)(5,10,15,20-tetraphenylporphinato)zinc(II) (hereafter **1**), which is reported herein, demonstrates the capability of a zinc atom to bind two axial ligands and to occupy a position in the mean plane of a porphyrin ligand.

Crystals of **1** have found recent use as hosts in a series of EPR studies of spin-labeled metallotetraphenylporphyrins.⁹ The

Table I. Crystallographic Parameters and Refinement Results for Zn(TPP)(THF)₂

mol formula	C ₅₂ H ₄₄ N ₄ O ₂ Zn
mol wt	822.33
space group	<i>P</i> $\bar{1}$
data collen temp, °C	-130
<i>a</i> , Å	9.572 (1)
<i>b</i> , Å	11.115 (2)
<i>c</i> , Å	11.720 (3)
α , deg	102.71 (2)
β , deg	103.78 (2)
γ , deg	115.01 (1)
<i>V</i> , Å ³	1022
<i>Z</i>	1
<i>D</i> (calcd), g cm ⁻³	1.34
cryst dimens, mm	0.48 (100- $\bar{1}$ 00) × 0.11 (010-0 $\bar{1}$ 0) × 0.20 (001-00 $\bar{1}$)
radiation	Mo K α (λ = 0.71073 Å), graphite monochromator
μ , cm ⁻¹	6.58
scan type	θ -2 θ
2 θ range, deg	3.5-50
reflens	$\pm h, \pm k, l \geq 0$; 3613 (3178 with <i>I</i> > 2σ(<i>I</i>))
scan speed, deg min ⁻¹	variable (3-30)
data:parameter ratio	11.4
<i>R</i>	0.040
<i>R</i> _w	0.043
GOF	1.60
<i>g</i>	8.7 × 10 ⁻⁴
slope of normal prob plot	1.18

spin-labeled complexes incorporated bulky nitroxyl-bearing substituents that were attached to a pyrrole carbon atom of the porphyrin ring. EPR spectra indicated that in all cases the *z* axes of the transition metal **g** and **A** tensors adopted similar orientations relative to the faces of the host crystal. Since these *z* axes are known to be normal to the porphyrin plane in metalloporphyrins, these results suggested that the porphyrin planes of host molecules and dopant molecules were parallel.

The EPR spectra indicated, however, that the spin-labeled substituents adopted several different positions in the lattice.⁹ It therefore appeared that there was more than one way that the nitroxyl-labeled porphyrin could pack into the host crystal and that the steric effects of the host on the dopant were different in different orientations. The correlation between the metal-nitroxyl distance and the angle between the normal to the porphyrin and

- (1) (a) Colorado State University. (b) University of Colorado at Denver. (c) University of Denver.
- (2) Collins, D. M.; Hoard, J. L. *J. Am. Chem. Soc.* **1970**, *92*, 3761.
- (3) (a) Storm, C. B.; Turner, A. H.; Swann, M. B. *Inorg. Chem.* **1984**, *23*, 2743. (b) Storm, C. B. *J. Am. Chem. Soc.* **1970**, *92*, 1423.
- (4) See, for example: (a) Vogel, G. C.; Searby, L. A. *Inorg. Chem.* **1973**, *12*, 936. (b) Vogel, G. C.; Stahlbush, J. R. *Inorg. Chem.* **1977**, *16*, 950. (c) McDermott, G. A.; Walker, F. A. *Inorg. Chim. Acta* **1984**, *91*, 95. (d) Lambert, P. *Chem. Commun.* **1967**, 470.
- (5) Gust, D.; Neal, D. N. *J. Chem. Soc., Chem. Commun.* **1978**, 681.
- (6) Scheidt, W. R.; Kastner, M. E.; Hatano, K. *Inorg. Chem.* **1978**, *17*, 706.
- (7) Braut, D.; Rougee, M. *Biochemistry* **1974**, *13*, 4591.
- (8) Reed, C. A.; Mashiko, T.; Scheidt, W. R.; Spartalian, K.; Lang, G. J. *Am. Chem. Soc.* **1980**, *102*, 2302.
- (9) (a) Damoder, R.; More, K. M.; Eaton, G. R.; Eaton, S. S. *J. Am. Chem. Soc.* **1983**, *105*, 2147. (b) Damoder, R.; More, K. M.; Eaton, G. R.; Eaton, S. S. *Inorg. Chem.* **1983**, *22*, 2836. (c) Damoder, R.; More, K. M.; Eaton, G. R.; Eaton, S. S. *Inorg. Chem.* **1983**, *22*, 3738. (d) Damoder, R.; More, K. M.; Eaton, G. R.; Eaton, S. S. *Inorg. Chem.* **1984**, *23*, 1320. (e) Damoder, R.; More, K. M.; Eaton, G. R.; Eaton, S. S. *Inorg. Chem.* **1984**, *23*, 1326.